Influence of Mechanical Stress and Surface Interaction on the Aggregation of *Aspergillus niger* Conidia

L.H. Grimm, S. Kelly, I.I. Völkerding, R. Krull, D.C. Hempel

Institute of Biochemical Engineering, Technical University of Braunschweig; telephone: +49-(0)531/391-7650; fax: +49-(0)531/391-7652; e-mail: d.hempel@tu-bs.de

Received 7 April 2005; accepted 23 June 2005

Published online 27 October 2005 in Wiley InterScience (www.interscience.wiley.com). DOI: 10.1002/bit.20666

Abstract: Productivity of fungal cultures is closely linked with their morphologic development. Morphogenesis of coagulating filamentous fungi, like *Aspergillus niger*, starts with aggregation of conidia, also denominated as spores. Several parameters are presumed to control this event, but little is known about their mode of action. Rational process optimization requires models that mirror the underlying reaction mechanisms. An approach in this regard is suggested and supported by experimental data. Aggregation kinetics was examined for the first 15 h of cultivation under different cultivation conditions. Mechanical stress was considered as well as pH-dependent surface interaction. Deliberations were based on a two-step aggregation mechanism. The first aggregation step is only affected by the pH-value, not by the fluid dynamic conditions in the bioreactor. The second aggregation step, in contrast, depends on the pH-value as well as on agitation and aeration induced power input. For the given experimental set-up, agitation had much more influence than aeration. In addition, hyphal growth rate was determined to be the driving force for the second aggregation step.

INTRODUCTION

Numerous biotechnological production processes are based on the submerse cultivation of filamentous fungi (Grimm et al., 2004a; Papagianni, 2004; Punt et al., 2002). Process design, however, is often hampered by the complex growth pattern of these organisms. There is an entangled relationship between productivity of fungal cultures and the morphologic development, which is affected by several cultivation parameters (Kelly et al., 2004). Many of these parameters are still chosen empirically due to lacking knowledge about the mechanisms governing the morphologic development.

In the past decades much effort has been paid to describe the formation of single fungal mycelia. Due to digital image analysis data (Cox, 1998), this has successfully led to elaborate models based on tip elongation and branching (Yang et al., 1992). Investigation of the intracellular control of morphogenesis has just begun, but should eventually allow detailed understanding of the effect of medium composition on hyphal growth (McIntyre et al., 2001). Several extracellular factors influencing fungal morphology have been determined. Power input into the bioreactor is probably one of the most important parameters, causing the mechanical stress responsible for hyphal breakage (Amanullah et al., 2002; Mitard and Riba, 1988). Hyphae chipped of the mycelium are able to keep on growing and thereby form new separate mycelia.

For a proper description of this phenomenon it is necessary to move from the observation of single mycelia to the characterization of mycelial populations. An approach therefore has been to postulate a general population balance equation (Nielsen and Krabben, 1995). Assuming that the number of tips and the total hyphal length are independent variables a two dimensional number density function is obtained. Generation of new elements was derived from hyphal fragmentation and the germination of conidia (Nielsen, 1993). Yet the starting conditions for coagulating organisms in this trend setting model need to be specified.

The beginning number of particles in solution corresponds to the amount of conidia used for inoculation, if coagulation is omitted. In the case of conidial aggregation the portion of submerged particles may vary considerably even before germination and hyphal fragmentation. A phenomenological description of conidial aggregation was published by (Metz and Kossen, 1977). Filamentous fungi were classified into coagulating and non-coagulating types according to their ability to form aggregates. A large number of variables influencing fungal aggregation processes have been published (Amanullah et al., 2001; El-Enshasy et al., 1999; Fujita et al., 1994; Tronchin et al., 1995). Most studies dealing with this issue have drawn conclusions from the morphology of full-grown mycelia. The amount of pellets in solution and the ratio of pellets to free mycelia can be attributed to conidial aggregation to a certain extent. Many parameters influencing this process also act upon hyphal growth, though, and it has been difficult to quantify their effect on aggregation alone.

Correspondence to: D.C. Hempel
Contract grant sponsor: German Research Foundation

A method for direct examination of conidial aggregation has been presented recently (Grimm et al., 2004b). Kinetic studies were performed with a particle size analyzer suggesting that at least two distinct aggregation steps had to be considered. Based on these findings the influence of significant process parameters may be investigated to determine their magnitude. The influence of initial conidial concentration on the aggregation process was determined this way (Grimm et al., 2004b). Further process parameters affecting conidial aggregation need to be analyzed. With about 5 μm diameter conidia are located on a boundary where particles may still be subject to mechanical forces but surface properties gain predominant control of their physical behavior (Li et al., 2004).

It is therefore important to characterize the hydrodynamic conditions of the bioreactor to assess the impact of mechanical stress on the aggregation process. The consequent task is to map the dependency of kinetic constants on the volumetric power input as a key variable of fluid dynamics. In case of turbulent flow the size of the smallest eddies is interesting as there is already evidence that it plays a decisive role on hyphal fragmentation (Cui et al., 1997). In relation to surface properties and their bearing on fungal morphology one of the most important process parameters is probably the pH-value (Carlsen et al., 1996; Galbraith and Smith, 1969). The electric charge of the macromolecules building up the conidial cell wall depends on the proton concentration in the surrounding medium. Highly charged particles are expected to repel one another. Despite controversial opinions on the importance of particle interaction forces for the conidial aggregation process, electrostatic effects are probably relevant (Dynesen and Nielsen, 2003). In this article research is focused on the influence of hydrodynamic conditions and pH-values on kinetic constants.

MATERIALS AND METHODS

Strain and Media

The model organism used in all experiments was *Aspergillus niger* AB 1.13. This is a protease deficient, uridine auxotroph, glucoamylase producing strain (Mattern et al., 1992). Conidia were obtained from *Aspergillus niger* cultures on 4 % (w/v) potato dextrose agar (PDA) with 0.1 % (w/v) uridine grown at 30°C for 5 days. Harvest was carried out by flooding the agar plates with sterile NaCl solution (0.9 % w/v) and scraping the aerial mycelium. Cell concentrations were determined from the optical density (OD) of the suspension measured at 600 nm. The values proved to correlate well with manual cell counts (Grimm et al., 2004b).

Composition of the defined Emmler medium used for aggregation assays was (in g/L): glucose monohydrate, 22.0; uridine, 0.244; $(NH_4)_2SO_4$, 1.65; KH_2PO_4, 2.5; $MgSO_4 \cdot 7\ H_2O$, 0.2; $CaCl_2 \cdot 2\ H_2O$, 0.1 and 0.1 mL/L trace element solution containing (in g/L): $ZnSO_4 \cdot 7\ H_2O$, 50; $Fe(NH_4)_2(SO_4)_2 \cdot 6H_2O$, 10; $CuSO_4$, 1.6; $Na_2MoO_4 \cdot 1\ H_2O$, 0.5; $MnSO_4 \cdot 1\ H_2O$, 0.5.

Cultivation

Cultivation of *Aspergillus niger* AB 1.13 was performed for 60 h in a standard 2L-bioreactor (Applikon, Netherlands) stirred with two six-blade impellers. Previous to inoculation an aqueous solution of glucose and uridine was sterilized inside the reactor. A salt and trace element solution was sterilized separately to prevent precipitation and added to the sterile glucose solution to reach the final medium composition described above. Agitation rate was set to 200/min (equivalent to an agitation induced power input of 0.12 W/kg). A constant pH value was regulated by addition of 1 M NaOH or 1 M HCl, respectively. Depending on the experiment the pH value was chosen in the range of 4–7. Aeration rate was adjusted to 0.06 m^3/h (corresponding to 0.5 vvm) and the medium tempered to 30°C.

Inoculation was carried out with a suspension of conidia prepared as presented earlier to obtain a final concentration of 2×10^6 conidia per mL in the reactor. This concentration was verified by OD measurement of a sample immediately after inoculation. Further samples of 20 mL were taken in steps of 8–12 h. Cell dry weight (CDW) was measured gravimetrically and glucose concentration via HPLC analysis of the supernatant. Image analysis methods were employed for quantification of macro-morphologic data. A series of pictures was shot from all pellets in 5 mL solution. These pictures were analyzed digitally with image analysis software (KS300, Zeiss, Gemany) to provide information about pellet size (i.e., cross sectional area) and concentration. Furthermore glucoamylase concentration was determined in the supernatant of each sample to establish the level of productivity. Glucoamylase activity was determined by the PNPG method described by Withers et al. (1998).

Aggregation Assay

Conidial aggregation kinetics was studied with an inline particle size analyzer (FBRM D600, Lasentec), which gathers time dependent particle size distributions and concentrations. The working principle of the analyzer is based on laser scanning microscopy. A laser beam is focused to a spot rotating at constant angular velocity. Laser light is scattered back by particles crossing this spot. Reflected light is collected on a photodetector and chord lengths are calculated from the reflection time and the rotational speed of the laser spot providing a particle size distribution every minute. It has been demonstrated that the number of counts per second in the range of 0–500 μm chord length corresponds to the concentration of all particles in solution (Grimm et al., 2004b). The median value of the chord length distribution between 0 and 500 μm was observed for 20 h to calculate the growth rate of the aggregates.

Conidial aggregation was tracked with the particle size analyzer in the same 2L-bioreactor in which previous cultivations were performed. This process proved to be concluded about 15 h after inoculation. Two test series were accomplished with different volumes of medium. 1 L of medium was

stirred with one six-blade turbine impeller, whereas two of the same impellers were used to mix 2 L of medium. For the experiments sterile medium was tempered at 30°C like in the cultivation. Single process parameters were varied to test their influence on the aggregation process. Agitation rate was varied between 100 and 300/min corresponding to the range of 0.014–0.390 W/kg of agitation induced power input. To determine the influence of agitation induced power input, gas flow was turned off. This was possible as not much biomass growth takes place during conidial aggregation and within the first few hours after germination. No oxygen limitation was observed by measurement of dissolved oxygen. Aeration induced power input was studied with gas flow rates between 0 and 0.5 m^3/h at an agitation rate of 150/min. The pH was adjusted to the desired value between 3 and 8 with either 1 M NaOH or 1 M HCl. After recording the background signal of the particle size analyzer at the corresponding conditions the tempered medium was inoculated with a suspension of harvested conidia to give a concentration of 2×10^6/mL. A sample of 1 mL was taken immediately after inoculation to determine cell concentration from the measurement of OD. Furthermore some experiments were carried out in 0.3 and 0.5 L glass beakers stirred with the same six-blade turbine impeller as in the 2L-bioreactor.

Power Input

To determine agitation induced power input, the torque on the stirrer was measured. A weight was laid on a balance and adjusted with a string perpendicularly to a pivoted motor driving the stirrer. Weight measured on the balance was reduced with increasing agitation rates due to the force transferred by the string. The weight difference was used to calculate the torque. In a filled vessel power input was determined from the torque and the corresponding agitation rate. Friction was considered by repeating the measurement with an empty vessel and subtracting the blank value obtained. To verify the data, power input was also determined by measuring the electric power consumption of the motor. This was done with a power measuring device switched between plug and power-socket (Energie-Check, 3000, Voltcraft, Germany).

The fluid dynamic conditions in the bioreactor are characterized by the Reynolds and the Newton (Power) number denominated as Re and Ne. Their definition is given in Equation 1 and 2 respectively. P is the agitation induced power input obtained from the experiments described before, where the agitation rate n was adjusted. The values for dynamic viscosity η and density ρ correspond to those of water. The impeller diameter d was 45 mm.

$$\mathrm{Re} \equiv \frac{n \cdot d^2 \cdot \rho}{\eta} \tag{1}$$

$$\mathrm{Ne} \equiv \frac{P}{\rho \cdot n^3 \cdot d^5} \tag{2}$$

For the experimental set-up used, aeration induced power input proved to have a negligible effect on the conidial aggregation process as will be shown later. Therefore it was not further described.

Zeta Potential

The zeta potential is probably the most popular parameter to characterize charged colloidal particles in suspension. It is given by the electric potential at the shear plane, an imaginary surface separating the layer of liquid bound to the particle and the rest of liquid showing normal viscous behavior. It therefore depends on the surface charge density and determines the stability of dispersions.

The zeta potential of conidia was determined at different pH-values. To remove large particles, which might clog the measuring chamber, the suspension of harvested conidia was filtered with gauze of 20 μm mesh size. After measuring the conidial concentration of the filtrate, it was used for the inoculation of each sample of 100 mL volume to a final concentration of 2×10^6/mL. Eleven samples were prepared this way, and the pH was adjusted between values of 3.0 and 8.0 in steps of 0.5. Zeta potential measurement of each solution was performed by electrophoresis (Zetamaster, Malvern, UK).

MATHEMATICAL MODEL

Conidial aggregation has been described as a process consisting of two distinct steps (Grimm et al., 2004b). The first step starts immediately after inoculation of a reactor with conidia. Two of these particles meet and form an aggregate. For the kinetic description of this process a simple general reaction is assumed as shown in Equation 3.

$$2N \underset{k_{-1}}{\overset{k_{+1}}{\rightleftharpoons}} N_2 \tag{3}$$

Subsequently particles are denominated as N in this case and one particle N_2 is formed as a cause of aggregation. The velocity of this reaction is determined by the kinetic constant k_{+1}. The aggregate may be also broken into its constituents, an event characterized by the constant k_{-1}. The time dependant development of particle concentration therefore involves two components describing formation and decomposition of aggregates. For a situation of steady state, in which the amount of aggregates does not vary, the condition of Equation 4 is fulfilled.

$$-\frac{\mathrm{d}N}{\mathrm{d}t} = k_{+1} \cdot N^2 - k_{-1} \cdot N_2 = 0 \tag{4}$$

N and N_2 are given by the concentration of the corresponding particles. The amount of particles in solution can be measured and the number of aggregates N_2 correlates with the difference between the initial concentration N_0 at the beginning of the aggregation process and the particle concentration N at steady state conditions. The aggregation constant K combines the kinetic constants k_{+1} and k_{-1} and

may be calculated according to Equation 5.

$$K = \frac{k_{-1}}{k_{+1}} = \frac{N^2}{N_0 - N} \tag{5}$$

Variation of process parameters is thus expected to influence K. The consequent task is to establish dependency functions. In addition, the mode of action of process parameters should be examined. Mechanical stress, for instance, is caused by the fluid dynamic conditions and transmitted by eddies. The size of the smallest eddies is given by the so-called Kolmogorov micro scale of length (Kusters, 1991). It is represented by r in Equation 6, where η is the dynamic viscosity of the liquid, ρ the density and ϵ the specific power input ($\epsilon = P/(V \cdot \rho)$).

$$r = \left(\frac{\eta^3}{\rho^3 \cdot \epsilon}\right)^{1/4} \tag{6}$$

The second aggregation step is presumably triggered by germination and hyphal length growth as new emerging surface is available for the attachment of conidia. The exponential length growth of germ tubes and hyphae in the early phase of mycelial growth is described by Equation 7 with l_{hyp} as hyphal length at the time t and μ as specific hyphal length growth rate.

$$\frac{dl_{hyp}}{dt} = \mu \cdot l_{hyp} \tag{7}$$

Separation of variables and integration of the differential equation in the boundaries of $l_{hyp,0}$ representing particle length at the beginning of the aggregation process (with $t = 0$) and l_{hyp} at the time t yields Equation 8.

$$l_{hyp}(t) = l_{hyp,0} \cdot e^{\mu \cdot t} \tag{8}$$

For simplification hyphae and germ tubes will be considered to be cylinders with a constant diameter d_{hyp} equivalent to the conidial diameter of about 5 μm. In this case, the increase in surface A_{hyp} over time due to hyphal length growth follows the definition of Equation 9.

$$\frac{dA_{hyp}}{dt} = \pi \cdot d_{hyp} \cdot \frac{dl_{hyp}}{dt} \tag{9}$$

The variation of particle concentration N with increasing adhesion surface A_{hyp} is a decisive matter of the second aggregation step. Supposing that conidia attach to hyphae at random positions the simple differential Equation 10 can be formulated. The parameter b specifies the amount of conidia per area unit.

$$-\frac{dN}{dA_{hyp}} = b \tag{10}$$

Integration of Equation 10 leads to the relationship of particle concentration over hyphal surface. Some considerations on the aggregation process are necessary for the choice of proper integration boundaries. Starting conditions are established by the outcome of the first aggregation step, discernible by the particle concentration N_{SS} during the first steady state. Hyphal surface area is assumed to be zero at this time. Over the following process, particle concentration N decreases with the corresponding hyphal surface area A_{hyp}. The result of integration is presented in Equation 11, taking into account Equations 8 and 9.

$$\int_{N_{SS}}^{N} dN = N - N_{ss} = -b \cdot \pi \cdot d_{hyp} \cdot l_{hyp,0} \cdot e^{\mu \cdot t} \tag{11}$$

This function is derived over time to obtain the kinetic behavior of particle concentration.

$$-\frac{dN}{dt} = b \cdot \pi \cdot d_{hyp} \cdot l_{hyp,0} \cdot \mu \cdot e^{\mu \cdot t} = \mu(N_{SS} - N) \tag{12}$$

Concluding from Equation 12, the time dependent decrease of particle concentration is driven by the specific hyphal length growth rate μ. Experiments have shown that at the end of the second aggregation step a second steady state is reached, where all conidia in solution are attached to growing particles. The amount of aggregates at this steady state will be denominated N_{end}. Like K of Equation 5, it is a characteristic variable dependent on process parameters.

RESULTS

Cultivation

Cultivation of *Aspergillus niger* AB 1.13 was performed at different growth conditions. Various consequences are observed by variation of only one process parameter. In the example presented in Figures 1 and 2 the same strain was grown at the same inoculum level and in the same reactor under comparable hydrodynamic conditions. The course of biomass and glucose concentration over time is depicted in Figure 1 for cultivations at pH values of 4 and 7. In this range of pH values biomass growth and substrate turnover prove to proceed at higher rates for lower pH values. This was

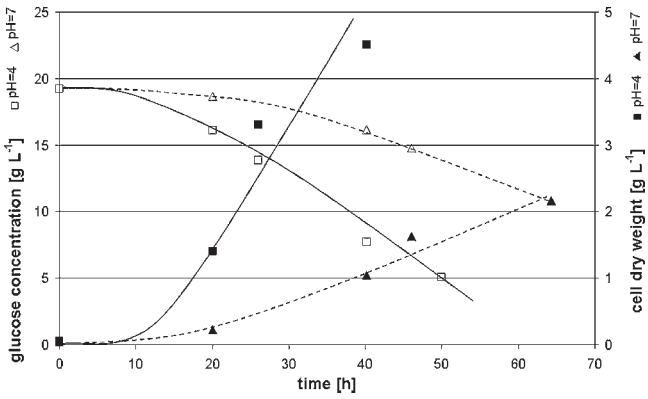

Figure 1. Development of biomass and carbon source concentration over cultivation time. *Aspergillus niger* AB 1.13 was growth in a 2L-bioreactor at an agitation rate of 200/min, an aeration rate of 0.06 m^3/h and pH 4 (—) as well as pH 7 (- - -).

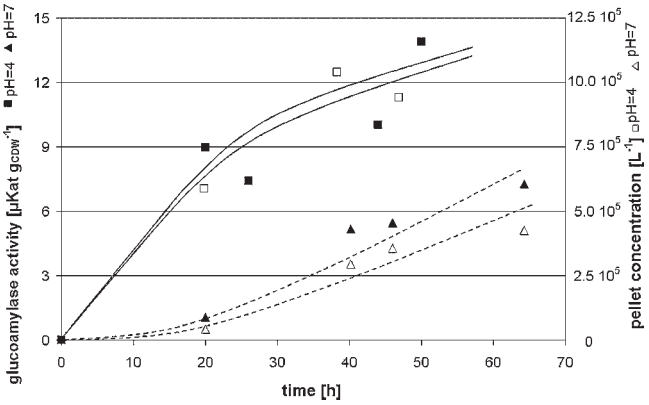

Figure 2. Product concentration in the supernatant per unit biomass and amount of pellets per Liter medium. Cultivation was performed in a 2L-bioreactor at an agitation rate of 200/min, an aeration rate of 0.06 m^3/h and pH values as in Fig 1.

supported by further experiments at other pH values (data not shown).

The impact on productivity may be evaluated from Figure 2. It features the level of glucoamylase activity in the supernatant per unit biomass accounting for the different development of CDW shown in Figure 1. Anyhow productivity per biomass is much lower at pH 7 than at pH 4. An explanation may be found in the fungal metabolism as substrate turnover was found to be lower at a pH value of 7. At the same time fungal morphology needs to be considered. Under the cultivation circumstances (low power input, moderate pH value and inoculum concentration) pellet growth was obtained.

Pellet concentration is plotted over cultivation time in Figure 2. At pH 4 the number of pellets in suspension is several times higher than at pH 7, although the same amount of conidia was used for inoculation. For both pH values, the time dependant course of pellet concentration resembles that of product per biomass, albeit data stems from independent measurements. The comparison of pellet concentration at pH 4 and at pH 7 yields a ratio, which is comparable to the relationship of product per biomass at these different pH values. All this is evidence for the influence of morphology on fungal productivity. Apparently a higher productivity is reached with an increasing amount of pellets in suspension.

The importance of morphogenesis is highlighted by these results. According to the time course of pellet concentration in Figure 2, morphological development proceeds over the entire cultivation time. Apparently, the amount of particles in solution increases over the cultivation process. Hyphal breakage leads to a continuous formation of new mycelia, which grow to form new pellets. This phenomenon has been vastly discussed in literature, but data on the processes of pellet formation is scarce. A two to three fold increase of pellet concentration was observed in Figure 2, but no information is available for the first 20 h, were particle concentration decreases from 2×10^9 conidia/L to about 10^5 pellets/L. This decrease of 4 orders of magnitude plays a decisive role in respect to the event of macro morphology (i.e., formation of pellets or free mycelia) and for the outcome of cultivation, as shown in Figure 2.

Analysis and description of the conidial aggregation process-taking place during the first 15 h of cultivation is therefore a major topic of research. The aggregation process was monitored with an online particle size analyzer, delivering sufficient data for a statistically sound scrutiny without the necessity of taking samples. The method has been verified by image analysis of samples as published (Grimm et al., 2004b). The number of counts per second in the range of 0–500 µm chord length corresponds to the total particle concentration in suspension. The time dependant development over the first 15 h of cultivation is exemplified in Figure 3, where a measurement in 1 L medium without aeration is illustrated. The pH-value was adjusted to 4.8, the agitation rate to 175/min and the initial conidial concentration to 2×10^6/mL. For all experiments two separate aggregation steps can be distinguished. The first one takes place immediately after inoculation and leads to a steady state within the first hour of cultivation. About 5–7 h later conidia begin to germinate. Starting from this time a second aggregation step is observed, which takes several hours and ends with a second steady state.

A simple mathematical model was drafted to fit this phenomenological description. It is based on a set of three kinetic constants, which describe the different aggregation steps. The effect of process parameters on these kinetic constants was determined. This might eventually allow influencing conidial aggregation by means of process engineering. This should primarily be possible through mechanical forces acting through hydrodynamics or by pH induced surface forces. Power input and pH are therefore the main variables examined throughout the following experiments. A brief characterization of fluid dynamics in the bioreactor and a description of the influence of pH value on the surface charge appear adequate before presenting their influence on conidial aggregation.

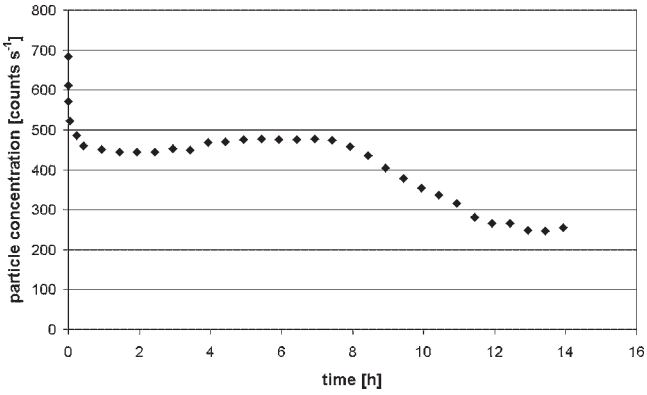

Figure 3. Particle concentration over time detected by particle size analyzer in counts per second between 0 and 500 μm. 1 L medium was inoculated with conidia to a final concentration of 2×10^6/mL. Agitation rate was set to 175/min without aeration and pH adjusted to 4.8.

Fluid Dynamics

The fluid dynamic conditions in the bioreactor are characterized by the Re- and the Ne-number (see Eqs. 1 and 2). The power input P was determined mechanically from the torque on the stirrer and with an electric power measuring device. Both methods provide similar results as presented in Figure 4. The Newton number converges towards a constant value of about 8 with increasing Reynolds numbers. A constant Newton number is evidence for turbulent flow conditions. Under those circumstances a typical Newton number of 5 is expected starting from Reynolds numbers of about 1×10^4. In our case a higher constant Newton number was detected beyond Reynolds numbers of 2×10^4. These values are dependent on the geometric set-up though, which explains the slight difference to expected values. The range of Reynolds numbers observed corresponds to the agitation rates at which aggregation occurs. Evidently, this is the case during the transition of laminar to turbulent flow and under early turbulent flow conditions.

Surface Properties

Besides power input pH may also influence the aggregation of conidia by modifying their surface charge. The zeta potential of conidia was studied to confirm that the electric potential in the shear plane changes with the pH-value. This is illustrated in Figure 5. A negative zeta potential was found for all samples examined. It decreases steadily with pH starting with about −6 mV at pH 3 until −22 mV at pH 8. Surface charge is therefore concluded to be higher for increasing pH-values. The absolute zeta potential measured is lower than that of most bacteria.

Published values lie between −23.8 mV for *B. cereus* and −31.3 for *E. coli* at pH 7 (Krekeler, 1991). This may be one reason for conidial aggregation. Electrostatic repulsion forces are subsequently less pronounced for *Aspergillus niger* conidia than for most bacteria. On the other hand an influence of surface charge on aggregation has to be rendered possible, because of the presence of a zeta potential as low as

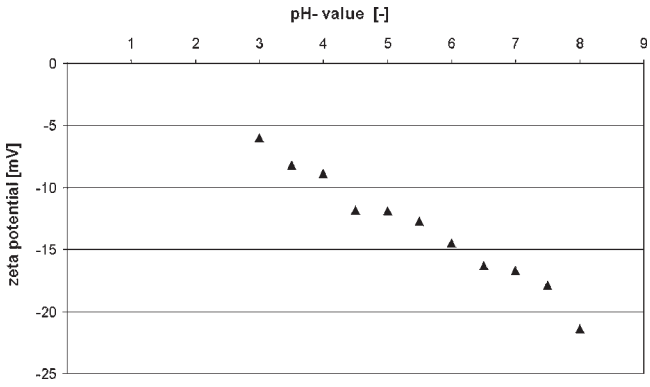

Figure 5. Zeta potential of conidia at different pH-values.

it may be. Thus aggregation assays were performed in 2 L medium with a conidial concentration of 2×10^6/mL. As the impact of different pH-values on aggregation was unclear, experiments were carried out at different agitation rates. If mechanical forces outweighed interparticle forces, an effect would only be visible at very low power input.

Kinetic Constants

According to Equation 5 the aggregation constant K is calculated from the mean particle concentration found during the first steady state conditions and the initial particle concentration measured by the particle size analyzer immediately after inoculation. This constant was calculated for different aggregation assays carried out under conditions equivalent to those of the cultivation presented earlier. The agitation induced power input and the pH value were varied. Results are given in Figure 6. A clear relationship between the constant K and the proton concentration of the medium was observed. With increasing pH, values of K became smaller steadily. This effect is less pronounced with higher pH.

Agitation induced power input apparently does not affect the constant K for the first aggregation step. An explanation may be provided by the Kolmogorov micro scale of length. It

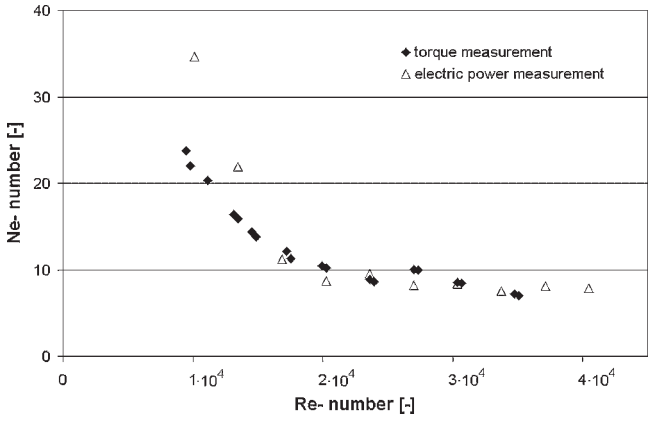

Figure 4. Fluid dynamics in a 2L-bioreactor without aeration. The Newton number was determined with two alternative methods and plotted over the Reynolds number adjusted for each measurement.

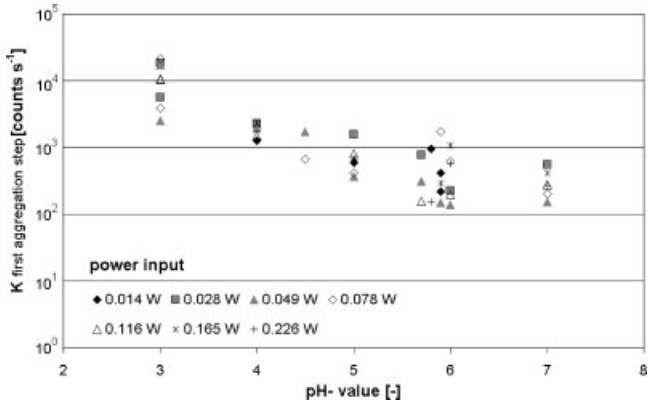

Figure 6. Aggregation constant K for the first aggregation step in 2L medium for different pH values and agitation rates between 100 and 250/min.

was calculated from Equation 6 for each power input of Figure 4. The micro scale of length is equivalent to the size of the smallest eddies in solution assuming turbulent flow. This is the case for high agitation rates. At low power input fluid dynamics is still in transition from laminar to turbulent flow as presented earlier. This condition is difficult to describe, but eddy sizes are certainly not smaller than the Kolmogorov micro scale of length. The length calculated therefore represents the minimum value possibly reached. It does not fall below 40 μm in the examined range of power input, relevant for conidial aggregation. This means that conidia and most aggregates are smaller than the smallest eddies, if a conidial diameter of 5 μm is estimated.

The constant N_{end} corresponds to the particle concentration at the end of the second aggregation process, were all conidia are bound to growing particles and a new steady state is reached (cp. Figure 3). The value of N_{end} was monitored for different cultivation conditions in order to characterize the second aggregation step. As demonstrated in Figure 7, pH has a bearing on the second steady state as well. A decreasing amount of stable particles was observed with increasing pH values. Higher values of N_{end} were obtained at a certain pH value, when power input was raised. The overall effect of pH on N_{end} proved to be more pronounced, though, especially for low pH values. At higher pH, the values of N_{end} were rather low and decreased less.

In contrast to the first aggregation step, where the collision of conidia is presumed to be responsible for the process, the second aggregation step is probably triggered by germination and hyphal length growth. This leads to a major increase in particle size beyond the Kolmogorov micro scale. The parameter N_{end} was defined to be the total particle concentration at the second steady state, when all conidia are thought to be bound to stable aggregates. This may explain why power input apparently affects N_{end} to some extend in contrast to the constant K. An increasing amount of particles is observed with mounting power input probably due to rising mechanical stress and particle breakage.

Despite the convenience of using steady state parameters like K and N_{end}, a thorough description of the aggregation

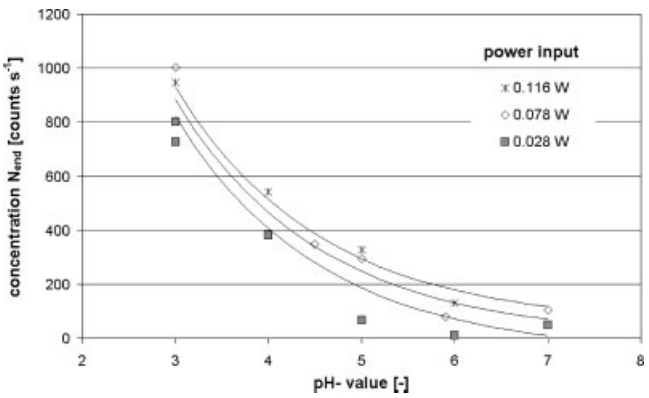

Figure 7. Concentration N_{end} at the second steady state over the pH-value. Cultivations were performed without aeration in 2 L medium at different agitation rates.

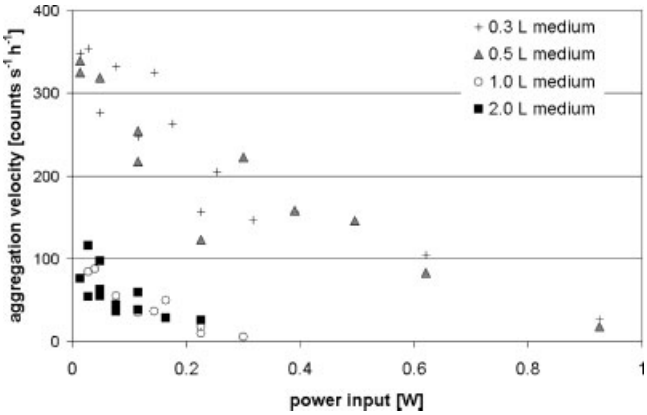

Figure 8. Velocity of the second aggregation step under varying agitation induced power input in different reaction vessels: 0.3 and 0.5 L glass beakers and 2L bioreactor filled with 1 and 2L medium.

process also needs to consider the dynamic nature of aggregation. The aggregation velocity calculated from the slope of particle concentration over time provides a suitable value. The aggregation velocity of the second aggregation step was determined under various conditions for different experimental set-ups. The influence of fluid dynamics is found in Figure 8. Beside the experiments in the 2L bioreactor the second aggregation step was also tracked in glass beakers with working volumes of 0.3 and 0.5 L. In all vessels aggregation velocity diminished with increasing power input. In the glass beakers the level of aggregation velocity was equivalent regardless of the working volume. Maximal local power input brought into the reactor therefore seems to be the decisive variable, instead of the mean volumetric power input. In the 2L-bioreactor agitation rates were smaller but similar, too. In this case 1 L medium was mixed with one impeller and 2 L were mixed with two impellers. The additional power input supplied by the second impeller was apparently compensated by the larger volume. In regard to this discrepancy between the different reaction vessels the different flow fields have to be considered.

Power input by agitation has been presented. Aeration of the cultivation broth is another source of power input omitted so far. A test series was arranged to investigate the influence of aeration on conidial aggregation. The range of aeration rates analyzed corresponded to the values usually set during cultivation. The velocity of the second aggregation step is plotted over the aeration rate in Figure 9. With mounting gas supply a decrease of aggregation velocity was detected for an agitation rate of 150/min. Power input by aeration appears to have an impact on conidial aggregation, but less than agitation induced power input. While aggregation is almost inhibited at high agitation induced power input (cp. Figure 8), aggregation velocity is only reduced from 50 to 30 counts/s/h by gas flow.

Aggregation velocity was also examined at different pH-values in 2 L medium without aeration as displayed in Figure 10. The course of aggregation velocity is almost the same for all pH-values. It was approximated by regression resulting in comparable exponential slopes. The absolute

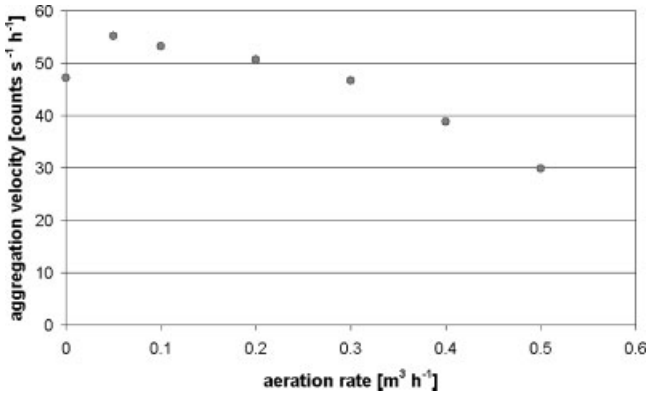

Figure 9. Velocity of the second aggregation step in 2 L medium at a constant agitation rate of 150/min with different aeration rates. The pH-value was adjusted to 4.8.

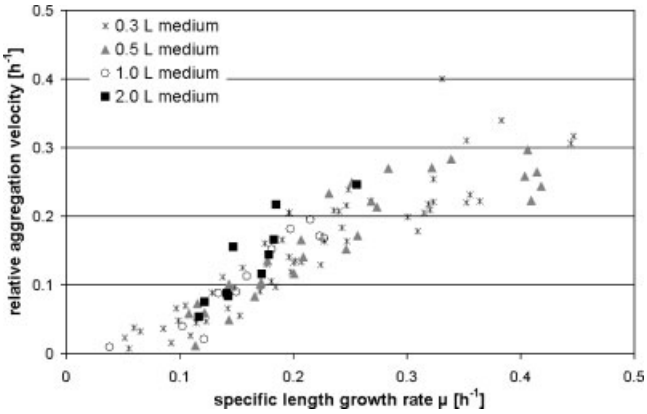

Figure 11. Relative aggregation velocity plotted against growth rate for aggregation assays under different growth conditions in various experimental set-ups.

value of aggregation velocity varies though. The highest velocities are reached at pH 4. With increasing pH the second aggregation step apparently runs slower.

Germination and growth of mycelia are expected to foster the second aggregation step. According to the model presumptions presented here, this aggregation step, taking place about 6–12 h after inoculation, would only depend on the hyphal length growth rate (see Eq. 9). This growth rate was determined from the exponential increment of the median value of the chord length distribution, recorded by the particle size analyzer. Various experiments were driven in different reaction vessels under changing agitation rates and initial particle concentrations. The aggregation velocity was related to the initial concentration N_{SS}, corresponding to the amount of counts per second in the first steady state. Figure 11 features the relative aggregation velocity in relation to the respective growth rate. A proportional dependency is visible for all data, regardless of power input, conidial concentration and reaction vessel used.

This was considered to be evidence for the validity of the model assumptions. Based on this finding the kinetic parameter b defined by Equation 10 was calculated. According to Equation 12 the velocity of the second aggregation step was related to a function of the hyphal length growth rate. The value of μ was determined from the increment of the median value of the chord length distribution for each experiment (cp. Figure 9). The diameter d_{hyp} and the starting particle length $l_{hyp,0}$ were estimated to be 5 μm. Results for b are given in Figure 12 in dependence of the specific agitation induced power input for different pH values. Like in Figure 8, b decreases with increasing power input and according to Figure 10 the value of b increases with decreasing pH value.

DISCUSSION

The main parameters adjustable during a cultivation process have been examined in respect to their behavior upon conidial aggregation. They act primarily through mechanical and interparticle surface forces. Mechanical stress is defined by the fluid dynamic conditions of the reaction vessel. The size of the smallest eddies represented by the Kolmogorov micro scale of length is thought to set a limit to the scope of fluid dynamic action. Evidence is provided by the given results. Aggregation of small conidia in the first aggregation step is apparently not influenced by the agitation-induced power input as demonstrated. The concentration N_{end}

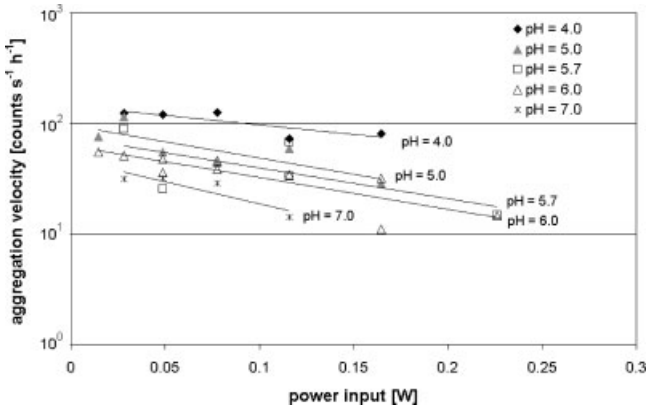

Figure 10. Velocity of the second aggregation step in 2 L medium without aeration at various pH-values and different agitation rates between 100 and 250/min.

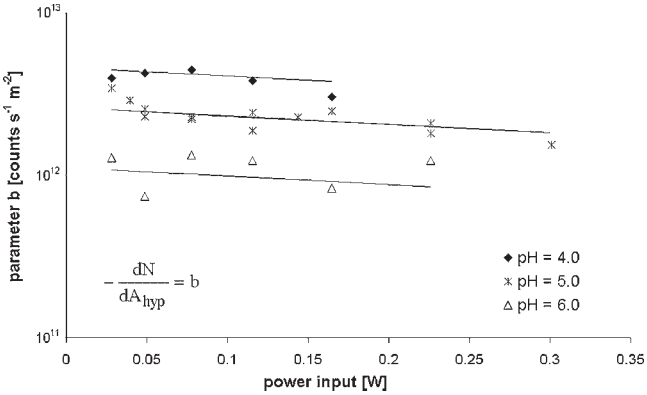

Figure 12. Parameter b calculated for the second aggregation step in relation to the specific agitation induced power input for different pH values.

measured after the second aggregation step, in contrast, is dependent on power input. The second aggregation step is involved with hyphal length growth and thus with larger particles. Increasing power input apparently leads to higher particle concentrations at the second steady state. This might be explained by mechanical stress working against aggregation and causing particle break-up.

The exact mechanism of mechanical stress on conidial aggregates still needs to be elucidated. It has to do with the fluid dynamic flow field as shown by the study of aggregation velocity in different reaction vessels. In the 0.3 and 0.5 L glass beakers additional volume did not change aggregation velocity, which implies that strain is primarily applied on aggregates in a distinct region probably close to the stirrer. On the other hand specific power input seems to be relevant for conidial aggregation in the 2L bioreactor with baffles, where additional regions of high stress may be present. Further insight might be provided by an extensive characterization of fluid dynamics in bioreactors. Modern techniques like particle image velocimetry (PIV) are available for this end. Knowledge on this matter is desirable all the more, as not only conidial aggregation but hyphal growth, branching, and fragmentation are also profoundly dependant on the mechanical stress in a bioreactor. Fluid dynamic characterization is essential especially for the development of large production plants.

The importance of aeration induced power input in this context needs to be pointed out. In the present study, aeration proved to play a minor role on conidial aggregation. Power input by aeration is caused by the ascension of bubbles, their expansion and velocity, all parameters affected by the hydrostatic pressure of the fluid column. In the 2L-bioreactor tested, the hydrostatic pressure is rather low. Therefore the effect of aeration on conidial aggregation may be much more pronounced in larger reaction vessels.

The second major aspect covered here dealt with the impact of surface forces on the conidial coagulation process. Priority was set on pH as an important adjustable process parameter. The expected relationship of the conidial zeta potential and the pH-value was established. It serves as explanation for the phenomena observed. The pH-value affects the first aggregation step as well as the second one. The movement of single conidia thus seems to be influenced by the surface charge. The aggregation constant K decreased with increasing pH. This is interesting as surface charge increases respectively and repulsion forces are thought to intensify. A large value of K is generated by high kinetic decomposition constants k_{-1} and low aggregation constants k_{+1}. For a solution to this inconsistence the energy field around a charged particle has to be considered. As electric forces are superposed by other forces, especially van-der-Waals forces, electric repulsion cannot be accounted for particle movement alone. A barrier caused by electric charge may still be overcome by particles with enough kinetic energy, but conidia bound once are shielded from foreign influence. As a result higher electric charge is expected to stabilize aggregates. This was noticed from the decrease of K with increasing pH. Less particles are consequently observed at higher pH-values not only after the first aggregation step, but also after the second one, as described by the parameter N_{end}. Furthermore, stabilization of the aggregation process with increasing pH leads to lower aggregation velocities and lower values of b.

A comprehensive description of the action of surface forces on the conidial aggregation process therefore needs to identify further variables. Especially hydrophobic interaction should be focused. It may well depend on the composition of the cell wall. Kinetic studies with cell wall mutants might allow further conclusions on this issue. The intracellular metabolism is certainly involved in the conidial aggregation at least the second step by affecting the hyphal length growth rate. Many processes leading to conidial germination and hyphal differentiation are still unknown. It will take some time to unfold mechanisms to modify them in the desired way either through genetic engineering or medium composition.

The consequence of conidial aggregation for fungal morphology has been portrayed by cultivations at different pH values. Twenty hours after inoculation the number of pellets in suspension is about 10 times higher at pH 4 than at pH 7. This finding matches the conclusions drawn about the conidial aggregation process. A pronounced decrease in particle concentration was already observed for low pH values during the first and the second aggregation step. Low growth rates at high pH values, as shown in Figure 1, have also been tracked with the particle size analyzer. They affect the second aggregation step according to Figure 11. Cultivation success and productivity are closely linked with morphologic development. The mathematic model presented in this article may offer some help to asses the influence of important process parameters on the early stage of morphogenesis. For a precise model conidia and hyphae still need to be distinguished and the number of conidia germinated over time is required. Such a population model of conidial aggregation should finally be integrated into a global population balance to describe the behavior of filamentous fungi for the course of a complete cultivation.

The authors gratefully acknowledge financial support provided by the German Research Foundation (DFG) through the collaborative research centre SFB 578-''From gene to product'' at the TU Braunschweig. Kind assistance was offered by the Institute of Sanitary and Environmental Engineering, TU Braunschweig, concerning the measurement of conidial zeta potential.

References

Amanullah A, Leonildi E, Nienow AW, Thomas CR. 2001. Dynamics of mycelia aggregation in cultures of Aspergillus oryzae. Bioproc Biosys Eng 24:101–107.

Amanullah A, Christensen LH, Hansen K, Nienow AW, Thomas CR. 2002. Dependence of morphology on agitation intensity in fed-batch cultures of Aspergillus oryzae and its implications for recombinant protein production. Biotech Bioeng 77(7):815–826.

Carlsen M, Spohr AB, Nielsen J, Villadsen J. 1996. Morphology and physiology of an alpha-amylase producing strain of Aspergillus oryzae during batch cultivations. Biotechnol Bioeng 49:266–276.

Cox PW. 1998. Image analysis of the morphology of filamentous microorganisms (review article). Microbiology 144:817–827.

Cui YQ, Lans RGJMvd, Luyben KCAM. 1997. Effect of agitation intensities on fungal morphology of submerged fermentation. Biotechnol Bioeng 55(5):715–726.

Dynesen J, Nielsen J. 2003. Surface hydrophobicity of Aspergillus nidulans conidiospores and its role in pellet formation. Biotechnol Prog 19(3):1049–1052.

El-Enshasy HA, Hellmuth K, Rinas U. 1999. Fungal morphology in submerged cultures and its relation to glucose oxidase excretion by recombinant Aspergillus niger. Appl Biochem Biotechnol 81(1):1–11.

Fujita M, Iwahori K, Tatsuta S, Yamakawa K. 1994. Analysis of pellet formation of Aspergillus niger based on shear-stress. J Ferment Bioeng 78(5):368–373.

Galbraith JC, Smith JE. 1969. Filamentous growth of Aspergillus niger in submerged shake culture. Trans Br Mycol Soc 52(2):237–246.

Grimm LH, Emmler M, Horn H, Krull R, Hempel DC. 2004a. Morphologie und produktbildung des pellet bildenden pilzes Aspergillus niger. Chem Ing Tech 76(9):1232.

Grimm LH, Kelly S, Hengstler J, Göbel A, Krull R, Hempel DC. 2004b. Kinetic studies on the aggregation of Aspergillus niger conidia. Biotechnol Bioeng 87(2):213–218.

Kelly S, Grimm LH, Hengstler J, Schultheis E, Krull R, Hempel DC. 2004. Agitation effects on submerged growth and product formation of Aspergillus niger. Bioproc Biosys Eng 26(5):315–323.

Krekeler C. 1991. Einfluss der Oberflächeneingenschaften von Mikroorganismen auf die Adsorption an porösen Trägermaterialien und deren Anwendung als Immobilisierungsmatrix [doctoral thesis]. Braunschweig: TU Braunschweig. 143p.

Kusters KA. 1991. The influence of turbulence on aggregation of small particles in agitated vessels [doctoral thesis]. Eindhoven: Technische Universiteit Eindhoven. 203p.

Li Q, Rudolph V, Weigl B, Earl A. 2004. Interparticle van der Waals force in powder flowability and compactibility. Int J Pharm 280(1–2):77–93.

Mattern IE, Noort JMv, Berg Pvd, Archer DB, Roberts IN, Hondel CAMJJvd. 1992. Isolation and characterization of mutants of Aspergillus niger deficient in extracellular proteases. Mol Gen Genomics 234:332–336.

McIntyre M, Mller C, Dynesen J, Nielsen J. 2001. Metabolic engineering of the morphology of Aspergillus. Adv Biochem Eng/Biotechnol 73:103–128.

Metz B, Kossen NWF. 1977. The growth of molds in the form of pellets—a literature review. Biotechnol Bioeng 14:781–799.

Mitard A, Riba JP. 1988. Morphology and growth of Aspergillus niger ATCC 26036 cultivated at several shear rates. Biotechnol Bioeng 32:835–840.

Nielsen J. 1993. A simple morphologically structured model describing the growth of filamentous microorganisms. Biotech Bioeng 41(7):715–727.

Nielsen J, Krabben P. 1995. Hyphal growth and fragmentation of Penicillium chrysogenum in submerged cultures. Biotech Bioeng 46(6):588–598.

Papagianni M. 2004. Fungal morphology and metabolite production in submerged mycelial processes. Biotechnol Adv 22:189–259.

Punt PJ, Biezen vN, Conesa A, Albers A, Mangnus J, Hondel CAMJJvd. 2002. Filamentous fungi as cell factories for heterologous protein production. Trends Biotechnol 20:200–206.

Tronchin G, Bouchara JP, Ferron M, Larcher G, Chabasse D, D. C. 1995. Cell surface properties of Aspergillus fumigatus conidia: Correlation between adherence, agglutination, and rearrangements of the cell wall. Can J Microbiol 41(8):714–721.

Withers JM, Swift RJ, Wiebe MG, Robson GD, Punt PJ, van den Hondel CA, Trinci APJ. 1998. Optimization and stability of glucoamylase production by recombinant strains of Aspergillus niger in chemostat culture. Biotechnol Bioeng 59(4):407–418.

Yang H, Reichel U, King R, Gilles ED. 1992. Measurement and simulation of the morphological development of filamentous microorganisms. Biotechnol Bioeng 39(1):44–48.